Development of intertidal flats in the Dutch Wadden Sea in response to a rising sea level
Spatial differentiation and sensitivity to the rate of sea level rise

Huismans, Ymkje; van der Spek, Ad; Lodder, Quirijn; Zijlstra, Robert; Elias, Edwin ; Wang, Zheng Bing

Important note
To cite this publication, please use the final published version (if applicable).
Please check the document version above.

Development of intertidal flats in the Dutch Wadden Sea in response to a rising sea level: Spatial differentiation and sensitivity to the rate of sea level rise

Ymkje Huismans [a,b,*], Ad van der Spek [b,d], Quirijn Lodder [a,c], Robert Zijlstra [c], Edwin Elias [b], Zheng Bing Wang [a,b]

[a] *Faculty of Civil Engineering and Geosciences, Delft University of Technology, 2600, GA Delft, the Netherlands*
[b] *Deltares, 2600, MH, Delft, the Netherlands*
[c] *Rijkswaterstaat, 3500, GE, Utrecht, the Netherlands*
[d] *Faculty of Geosciences, Utrecht University, P.O. Box 80115, 3508, TC, Utrecht, the Netherlands*

ARTICLE INFO

ABSTRACT

The Wadden Sea is a unique intertidal wetland area, forming an important hub for migratory water birds. A feared effect of accelerated sea-level rise (SLR) is the gradual loss or even disappearance of the ecologically valuable intertidal flats. To date, the effect of SLR on the time-evolution of the intertidal areas in the Dutch Wadden Sea has not been studied. To explore the sensitivity of the intertidal flats to SLR and the spatial differentiation of the response, simulations are carried out with the reduced-complexity model ASMITA for four sea level rise scenarios: one with a stable rate of 2 mm/yr (current rate), and three with accelerated sea level rise rates to respectively 4, 6 and 8 mm/yr. In addition, a scenario with a linearly increasing rate to 17 mm/yr in 2100 has been added to get an impression of what may happen under more extreme SLR-rates. The results show that the intertidal flats in the larger basins are most vulnerable to drowning. Due to differences in tidal flat geometry, the intertidal flats in the smaller basins mainly reduce in average height, while the intertidal flats in the larger basins mainly reduce in surface area. Within the basins, largest losses are expected to occur just off the land reclamation works and along the western part of each tidal watershed. The intertidal flats are sensitive to the rate of SLR. With doubling the rate of SLR, losses nearly double as well. Complete drowning is not predicted for any of the considered scenarios, but for the larger basins volume losses of nearly 50% by 2100 are predicted for the highest considered scenario. This will transform these basins into more lagoon-like basins, which is expected to have major consequences for the ecology.

1. Introduction

The Wadden Sea is one of the world's largest intertidal wetlands. The area spans nearly 500 km along the northern coast of the Netherlands and the North Sea coasts of Germany and Denmark (Fig. 1). It is a designated Nature 2000 site and inscribed on the UNESCO World Heritage List. The Wadden Sea forms an important hub for migratory water birds. From the water birds that use the East Atlantic flyway, at least 52 populations of 41 species use the Wadden Sea in internationally important numbers for breeding or wintering (Blew and Südbeck, 2005). A feared effect of accelerated sea-level rise (SLR) is the loss or even

disappearance of the ecologically valuable intertidal flats. As intertidal flats are the main feeding habitat for a large proportion of the water bird species in the Wadden Sea (Van Roomen et al., 2012), this may have large consequences for the bird populations. In the Yellow Sea population declines of about 5% per year is associated with the loss of nearly 30% of tidal mudflats and the general degradation in ecosystem quality (Studds et al., 2017). In the Eastern Scheldt, the loss of intertidal area is expected to have negative effects in the future on the number of shorebirds (Smaal and Nienhuis, 1992; Troost and Ysebeart, 2011).

Aside from the ecological consequences, a larger water depth and less intertidal area can have an impact on flood safety. The presence of

---

intertidal areas and in particular salt marshes help to protect against waves and storm surge, as well as from coastal erosion (Barbier et al., 2011; Reed et al., 2018 and references therein). Not only the intertidal areas, but the overall capacity for the bed to keep up with SLR may have large consequences for the design height of flood defences. If SLR is not accompanied by increased deposition, larger depths will result in waves with longer periods, greater amplitudes, and higher run-up. In addition, changes in depth and friction will affect tide, surge, and wave characteristics. In shallow seas, these non-linear feedbacks are estimated to lead to about 50% larger design heights, relative to design changes caused by SLR alone (Arns et al., 2017). So, both for ecology and water safety it is important to know to which extent the Wadden Sea is able to keep up with SLR.

When the sea level rises, the accommodation space for sediment increases, leading to an increase in sediment demand (Beets and Van der Spek, 2000). If more sediment is available, the sediment import rates will increase, as well as the sedimentation. Whether the system can keep pace with SLR mainly depends on the sediment availability and composition, basin size and past large-scale engineering measures. This is expressed in the *critical rate*. If the rate of SLR stays below the critical level, a new dynamic morphological equilibrium can be established, with a larger equilibrium depth (Lodder et al., 2019) and a decrease of intertidal flats. However, if the SLR rate exceeds the critical level, the Wadden Sea will eventually drown and intertidal flats will disappear (Lodder et al., 2019; Stive and Wang, 2003; Van Goor et al., 2003).

So far, only few studies have been conducted on the future development of the Wadden Sea. For the German Wadden Sea the future development of the Sylt-Rømø bight has been explored for two SLR-scenarios, with a process-based model (Becherer et al., 2018). For their medium SLR scenario (SLR rates increasing to 7 mm/year in 2050–2100), mild losses in intertidal area are predicted. For higher SLR rates (SLR rates increasing to 17 mm/year in 2050–2100) a transition to a lagoon-like system is predicted, with losing about 50% of the intertidal area. For the Dutch Wadden Sea, studies have mainly focused on estimating the critical SLR-rates for various tidal inlet systems in the Dutch Wadden Sea (Van Goor et al., 2003; Wang et al., 2018). These studies show that larger basins generally have smaller critical SLR-rates, meaning that they will be more vulnerable to drowning. Based on a combination of the long-term averaged rate of observed sedimentation and relative SLR-scenarios, 'Wang et al. (2018) made predictions for intertidal volume losses, which for their RCP 8.5 scenario are 38%.

This study builds upon Wang et al. (2018), by evaluating the transient development of the intertidal areas in each of the Dutch Wadden Sea tidal basins, which has not been done to date. The aim is to provide insight into how the process of drowning proceeds in time, how sensitive it is to the rate of SLR and which spatial differentiation may be expected.

In addition, volume losses are for the first time translated to losses in surface area and flat-height, as these are more relevant parameters for determining the consequences for ecology.

For modelling the long-term development of the Wadden Sea under the influence of multiple SLR rates, choice is made to use the reduced complexity model ASMITA (Aggregated Scale Morphological Interaction between Tidal inlets and the Adjacent coast) (Stive et al., 1998; Stive and Wang, 2003; Townend et al., 2016a, 2016b). This model is developed for predicting the long-term evolution of estuarine systems. By calculating the water motion and sediment dynamics on an aggregated time- and spatial scale, computational times largely reduce, allowing for multiple long-term model runs. Another benefit is that ASMITA is not hampered by the morphodynamic spin-up time, because it relies on the concept of morphological equilibrium (Dam et al., 2016). The morphodynamic spin-up time in process-based models is on the order of decades, which generally complicates making quantitative comparisons between modelled and observed volume changes on the timescale of decades to a century (Becherer et al., 2018). This also explains why process-based models so far have had limited success for predicting the effect of SLR on the morphodynamic development (Wang et al., 2018).

The ASMITA model has been applied to many cases, ranging from idealized tidal inlet cases (e.g. Lodder et al., 2019) to real cases like the Wadden (e.g. Kragtwijk et al., 2004; Van Goor et al., 2003; Wang et al., 2018), various estuaries in the UK (Rossington and Spearman, 2009; Rossington et al., 2011; Townend et al., 2016a) and a selection of worldwide estuaries for a global assessment of the future response of estuarine systems to SLR (Hinkel et al., 2013).

In this study we apply the ASMITA model for each of the six Dutch Wadden basins. In order to explore the sensitivity to the SLR rate, four sea level rise scenarios are explored: one with a stable rate of 2 mm/yr (current rate), and three scenarios with accelerated SLR rates, increasing from the current rate of 2 mm/yr to 4, 6 and 8 mm/yr. Based on the hypsometric curves for each basin, estimates are made for how volume changes translate to changes in surface area and average height. To get a first idea of the spatial differentiation within the basin, the understanding of tidal basin evolution under high rates of sea-level rise during the Mid-Holocene (8800–5800 year ago) is used.

2. Method

2.1. ASMITA models

The essence of ASMITA is that it considers the hydrodynamic and sedimentation processes on an aggregated scale. For this, the area of interest is subdivided into morphological elements. For a tidal inlet system, the schematization consists of three elements: the ebb-tidal
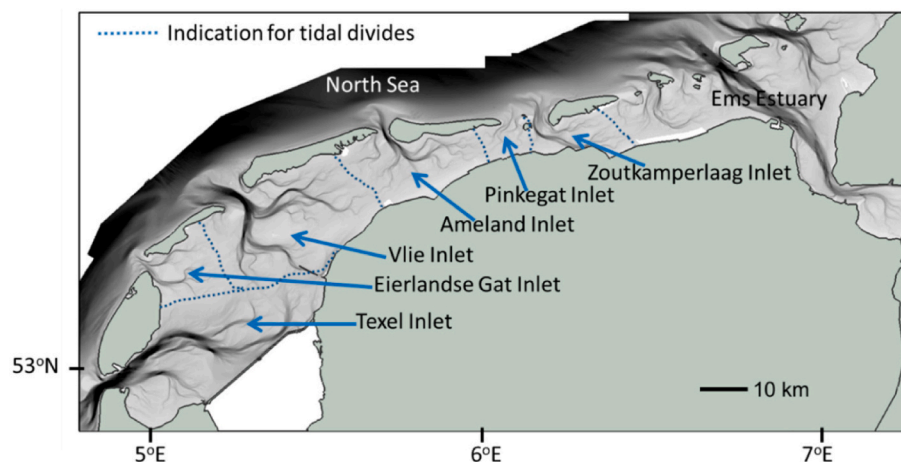

Fig. 1. Tidal basins in the Dutch Wadden Sea (after Lodder et al. (2019)).

delta, the channels and the intertidal flats, see Fig. 2. As a first step, the aggregated representation of the flow condition is calculated by determining the tidal prism. For each element, equilibrium relationships relating equilibrium volumes with tidal prism (ebb-tidal delta and channel) (Eysink, 1990) or tidal range (intertidal flats) (Renger and Partenscky, 1974; Eysink and Biegel, 1992) are used to determine the equilibrium volumes. The difference between the actual and equilibrium volume determines whether there is a sediment surplus or deficit. In case of a sediment deficit, the element will try to import sediment from a neighbouring element. The sediment availability, the exchange rate with the neighbouring elements and the vertical exchange rate with the bed in the element itself determine the resulting volume changes. Details on the equations and numerical schemes are given in (Townend et al., 2016a; Wang et al., 2020). How to relate the parameter settings on an aggregated scale to sediment parameters which can be measured in the field is elaborated in Wang et al. (2008), showing that these parameters are not merely calibration parameters.

In the course of time, various models have been setup for the Dutch Wadden tidal inlet systems. The first model, representing a typical Wadden inlet, was developed for studying the effects of subsidence within the framework of the first Environmental Impact Assessment study for gas extraction under the Wadden Sea (Buijsman, 1997; Eysink, 1998). Subsequently, Van Goor (2001, 2003) and Kragtwijk (2002, 2004), set up models for the individual basins of the Dutch Wadden Sea (see Fig. 1). Van Goor et al. (2003) studied the effect of SLR on Eierlandse Gat Inlet and Ameland Inlet. The same schematisation was used for the other inlet systems in the Dutch Wadden Sea (Bijsterbosch, 2003; Hinkel et al., 2013; Kragtwijk et al., 2004).

Based on newest insights from sediment budgets (Elias, 2006, 2019), the original parameter settings as derived by Kragtwijk (2002) have been updated twice (Lodder et al., Submitted; Z.B. Wang, Steetzel and Van Koningsveld, 2006). Lodder et al., (Submitted) used the updated model to study the impact of SLR on the sediment exchange through the tidal inlets, within the framework of Kustgenese 2 project. In this paper, we use the same model results for analysing the response of the intertidal areas to SLR. Details on the latest update on the parameter settings (Table 1.) are given in Lodder et al. (submitted).

2.2. Simulated scenarios

To explore the sensitivity of the intertidal flats to the rate of SLR and the spatial differentiation of the response, four scenarios are chosen: a reference scenario with a continuation of the present observed relative SLR rate and three scenarios with acceleration to 2, 3 and 4 times the present rate (Fig. 3). How the acceleration proceeds between present rate and final rate is based on the insights presented in Vermeersen et al. (2018). According to their analysis, the SLR rate increases linearly in time until the final rate is reached, which is the end of the acceleration period. The higher the final rate, the longer the acceleration period lasts. For the three acceleration scenarios considered, the acceleration ends in respectively 2050, 2060 and 2070. To preserve coherence with the present SLR rate at the Dutch coast, as reported by Baart et al. (2019) the

acceleration in our scenarios starts in 2020, and not earlier like the scenarios in Vermeersen et al. (2018). The chosen sensitivity scenarios (2–4 times the present rate) span the median sea level rise rates for Representative Concentration Pathways (RCP) 2.6 to just above RCP 4.5 in 2100 by Vermeersen et al. (2018). A fifth scenario, in which the sea level rise keeps accelerating to 17 mm/yr and with a total sea level rise in 2100 matching the RCP-8.5 scenario has been added to get an impression of what may happen under more extreme SLR-rates.

2.3. Analysis of model results for intertidal flat development

ASMITA calculates the volume changes of the morphological elements. For the development of the intertidal areas in response to SLR, it is relevant to know how this translates to changes in intertidal area and average flat height. To link the volume changes to changes in surface area and height, the hypsometric curves from the Wadden Sea inlets are used. A hypsomteric curve shows for each elevation how much surface area has an elevation at and below this level. For each tidal basin in the Wadden Sea, hypsometric curves have been derived by integrating the measured bathymetry over the entire tidal basin (Nederhoff et al., 2017). Based on the area and elevation occurring between mean low water level (MLW) and mean high water level (MHW), the volume of the intertidal flat can be calculated, and consequently the relation between volume, area and average height (=volume/area) can be derived, as illustrated in Fig. 4.

The values for MLW and MHW are derived from a combination of the mean sea level (MSL) from the "Zeespiegelmonitor 2018" (Baart et al., 2019) and the estimates for the average tidal range (Table 1):

For the translation of volume changes to area and height changes, the most recent available hypsometric curves are used, see Fig. 5. The results for the Zoutkamperlaag and Pinkegat inlets are combined, since no separate hypsometric curves are available.

Changes in flat volume in response to SLR, are caused by the change in MLW and sedimentation. To get an indication on how this relates to changes in flat area and height, the hypsometric curve is used as well (Fig. 4). The new volume is calculated by ASMITA. By assuming that the sedimentation is spread evenly on the intertidal area and no changes in the shape of the hypsometric curve occur, the hypsometric curve can be shifted upward by the amount of calculated sediment volume change. Combined with the changes in SLR, the to the new volume corresponding flat area and averaged flat height can be inferred. It is however likely that sedimentation is not spread evenly. To get an indication on how morphodynamic changes may change the relation between volume, area and average height, all available historic hypsometric curves as constructed by Nederhoff et al. (2017) have been used to derive a bandwidth reflecting historical variations, see Fig. 6.

For determining the intertidal area and volume from each historic hypsometric curve, first the MLW and MHW have been derived from the historic mean sea levels for Harlingen and Den Helder (Baart et al., 2009) and the tidal range. Note that for Ameland Inlet the bathymetric measurements from before 1970 are less reliable (Elias, 2019b) and therefore disregarded.


Fig. 2. *Schematization of a tidal inlet system into a 3-elements ASMITA model, with the ebb-tidal delta, channel and flats* (Lodder et al., submitted).

Table 1

Input parameters of the ASMITA application models for the tidal inlets, provided for reproducibility of the model results. Explanations of the parameters are given in the table. Full model formulation is given in Wang et al. (2020).

Inlet	Texel	Eierland	Vlie	Ameland	Pinkegat	Zoutkamp
Basic configuration: tidal range and the horizontal areas of the three elements: tidal range H and horizontal area A of the three elements. The subscripts indicate the elements, i.e. f = flat, c = channel, d = ebb tidal delta, which also apply to the following groups of parameters.						
H (m)	1.65	F(t)[a]	1.90	2.15	2.15	2.25
A_f (km^2)	133	105	328	178	38.1	65
A_c (km^2)	522	52.7	387	98.3	11.5	40
A_d (km^2)	92.53	37.8	106	74.7	34	78
Parameters influencing morphological timescale: n = power in the relation for the local equilibrium sediment concentration, C_E = global equilibrium concentration, w_s = vertical exchange coefficient in the element indicated by the second subscript, δ = horizontal exchange coefficient between the two elements indicated by the two subscripts (o = outside world).						
n (−)	2	2	2	2	2	2
C_E (−)	0.0002	0.0002	0.0002	0.0002	0.0002	0.0002
w_{sf} (m/s)	0.0001	0.0001	0.0001	0.0001	0.0001	0.0001
w_{sc} (m/s)	0.0001	0.00005	0.0001	0.00005	0.0001	0.0001
w_{sd} (m/s)	0.00001	0.00001	0.00001	0.00001	0.00001	0.00001
δ_{od} (m^3/s)	1550	1500	1770	1500	1060	1060
δ_{dc} (m^3/s)	2450	1500	2560	1500	1290	1290
δ_{cf} (m^3/s)	980	1000	1300	1000	840	840
Initial conditions: volumes of the three morphological elements in 1970						
V_{f0} (million m^3)	51.5	55	162	120	29.6	69
V_{c0} (million m^3)	2160	106	1230	302	18.5	177
V_{d0} (million m^3)	509.1	132	369.7	131	35	151
Parameters for defining the morphological equilibrium: V_{fe} = equilibrium volume of the flat element, α=coefficient in the relation between the equilibrium volume (V) of the element indicated by the subscript and the tidal prism (P): $V_{ce} = \alpha_c P^{1.55}$, $V_{de} = \alpha_d P^{1.23}$						
V_{fe} (million m^3)	87.78	57.83	250	131.2	30.3	70
α_c (10^{-6}) (m$^{-1.65}$)	15	13.13	9.6	10.241	10.14	27.266
α_d (10^{-3}) (m$^{-0.69}$)	4.025	8	2.662	2.92157	6.9278	9.137

[a] *For the Eierlandse Gat inlet the tidal range is set as function of time: it increases linearly from 1.73 m in 1970 with 3 mm per year.*
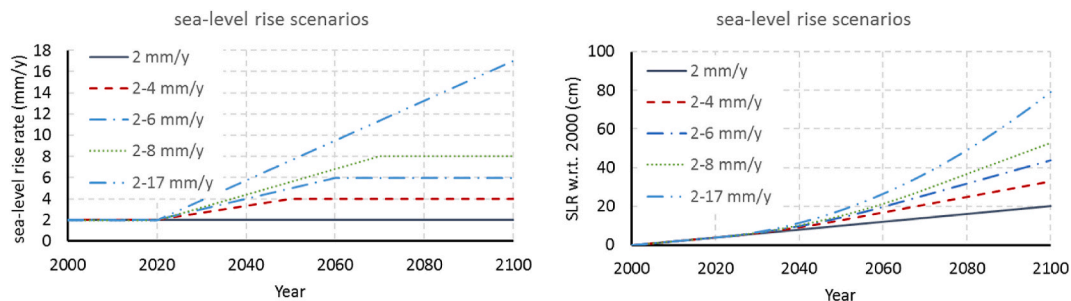
Fig. 3. The five sea-level rise scenarios considered in the present study. Left: change of SLR rate; right: SLR since 2000.

3. Model results

3.1. Sensitivity to the rate of sea level rise

The changes in intertidal flat area and average flat height in response to the four SLR scenarios are presented in Figs. 7 and 8. At a SLR rate of 2 mm/yr, all tidal inlets will be able to keep pace with SLR and show no loss of intertidal flat in 2100. The intertidal flat volume in the Marsdiep and Vlie inlet will even increase, as the sedimentation rate exceeds the rate of SLR. This effect is largest for the Marsdiep, with a final increase of 7% in intertidal volume. For all scenarios with accelerating SLR, the sedimentation rate is lower than the SLR rate, resulting in a loss of intertidal volume, area and height for all basins. For the most extreme scenario of 17 mm/yr, nearly half of the intertidal volume is predicted to disappear. It is furthermore noted that with an equal increase in SLR rate, a comparable extra loss of intertidal volume occurs. To illustrate, an increase in rate from 2 to 4 mm/yr leads to a loss of $1.8 \cdot 10^7$ m^3 in intertidal volume in the Vlie inlet, which is comparable to the extra loss of respectively $1.7 \cdot 10^7$ m^3 and $1.5 \cdot 10^7$ m^3 that occurs by increasing the rate from 4 to 6 mm/yr and from 6 to 8 mm/yr. Only a slight decrease in extra loss occurs with increasing SLR rate. This observation holds for all basins.

3.2. Spatial variation

The response of the intertidal flats differentiates per basin. The larger basins of the Texel Inlet (Marsdiep), Vlie Inlet and Ameland Inlet have most difficulty in keeping pace with SLR and show the highest volume losses (nearly 50%). Losses in the smaller inlets of Eierland, Pinkegat and Zoutkamperlaag stay limited to 19–30%. How the volume losses translate into losses in surface area and average height also differs per basin and is graphically illustrated in Fig. 9 for the SLR-17 scenario. For the larger basins the volume changes mainly translate into changes in surface area, while for the smaller basins they mainly translate into changes in average flat height. As a result, there is a strong differentiation between the basins in changes in surface area, with the largest loss of 43% ($15 \cdot 10^7$ m^2) in 2100 for the SLR-17 scenario for the Vlie Inlet and the smallest loss of 5% ($6 \cdot 10^6$ m^2) for the inlets of Pinkegat and Zouterkamperlaag. Less differentiation is observed for the change in average height, with the largest changes for the Vlie and Ameland Inlet of 22–23% (13–15 cm loss of average height) and smallest absolute changes for the Texel Inlet (19%, 9.1 cm).
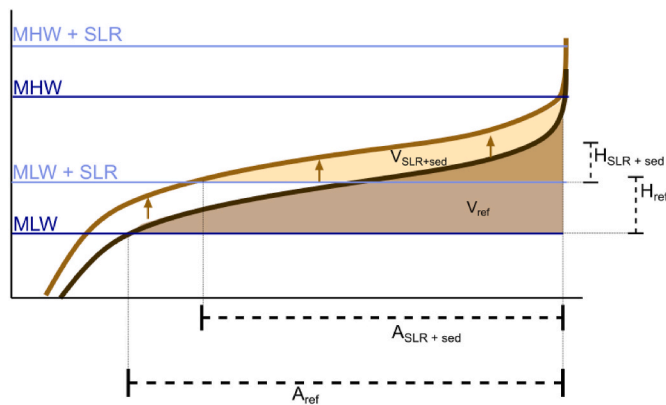
Fig. 4. Illustration of the method to derive the relation between intertidal flat volume, area and height from the hypsometric curve. The intertidal volume is defined as the volume between MLW and MHW, which is indicated by dark blue lines. From this the intertidal area and average flat height (H = V/A) is extracted. With SLR the tidal frame shifts up (light blue lines). In case sedimentation occurs, it is assumed to spread evenly over the system, such that the shape of the hypsometric curve will not change. The sedimentation is illustrated by the light brown arrows and curve. Volume, area and average flat height change accordingly. (For interpretation of the references to colour in this figure legend, the reader is referred to the Web version of this article.)

4. Discussion

### 4.1. Response to sea level rise

The variation in rate of SLR between the scenarios starts in 2020, resulting in corresponding differences in the development of the intertidal flat between these scenarios. The immediate differences in intertidal volume change per scenario reflect that it takes time before the

sedimentation rates change. Without changes in sedimentation rate, the changes in flat volume are a combination of the current sedimentation rate and the rate of SLR. So, the higher SLR-rates, the more volume losses occur. Only with time, the sedimentation rates increase, partially compensating the volumes losses induced by SLR. This delayed response of the sedimentation rates is in line with the observations of Lodder et al., (submitted) that the sediment transport through the inlets show a delayed response to SLR. This delay causes a sediment deficiency in the basins and a delay in sedimentation of the intertidal areas. In addition, with accelerating SLR a new dynamic equilibrium will be established, with a larger equilibrium depth (Lodder et al., 2019). With this, the sediment demand in the basins will also decrease, leading to less import. Both effects make the intertidal areas sensitive to SLR. The stronger the rate of SLR, the more losses occur. A slight decrease in response with further increase in SLR rate is noted, which means that with doubling the rate of SLR the losses nearly double as well. Note that, due to the variation in yearly averaged MSL with a bandwidth of about 5 cm (Baart et al., 2019; Vermeersen et al., 2018), the year to year variations in intertidal flat volume will be larger than the changes in response to SLR. Despite the sensitivity of the intertidal flats to SLR, it may subsequently take years to decades before changes in intertidal flat volume will become noticeable.

For the current most-extreme scenario, predicted volume losses range between 19% and 49% for 2100, with the largest losses for the largest basins. These numbers are in line with previous more crude estimates of Wang et al. (2018) of an average loss of 38% for the entire Dutch Wadden Sea. For the Sylt-Rømø beight in the German Wadden Sea, area losses of 50% are predicted, which is substantially more than the area losses predicted for the Dutch basins of similar size (26%–37%). However, their scenario of 17 mm/yr accelerates differently in time from present rate to final rate, leading to a total increase in sea level rise of 113 cm between 2010 and 2100. This is substantially more than median value of the RCP-8.5 scenario of about 80 cm between 2020 and
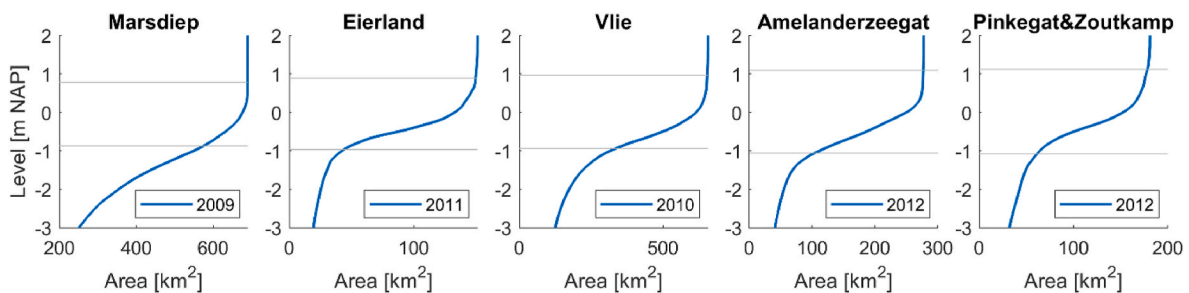
Fig. 5. Most recent hypsometric curves per inlet. The hypsometric curves are derived from in situ bathymetry (Nederhoff et al., 2017).
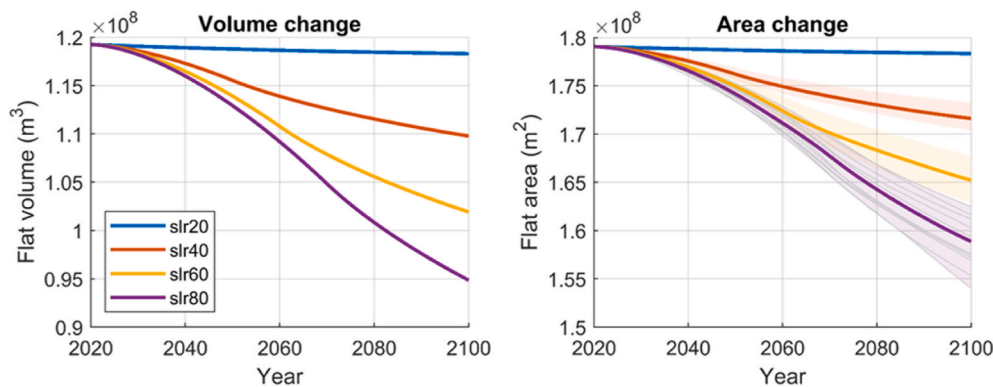
Fig. 6. Illustration on how changes in area relate to a given change in volume as determined by historic hypsometric curves (grey lines). Curves from before 2000 have been smoothed with a gaussian filter. The resulting bandwidth subsequently reflects the range of historical changes. Left: the calculated volume change, and right the related change in area. Method is illustrated for the slr80 scenario.
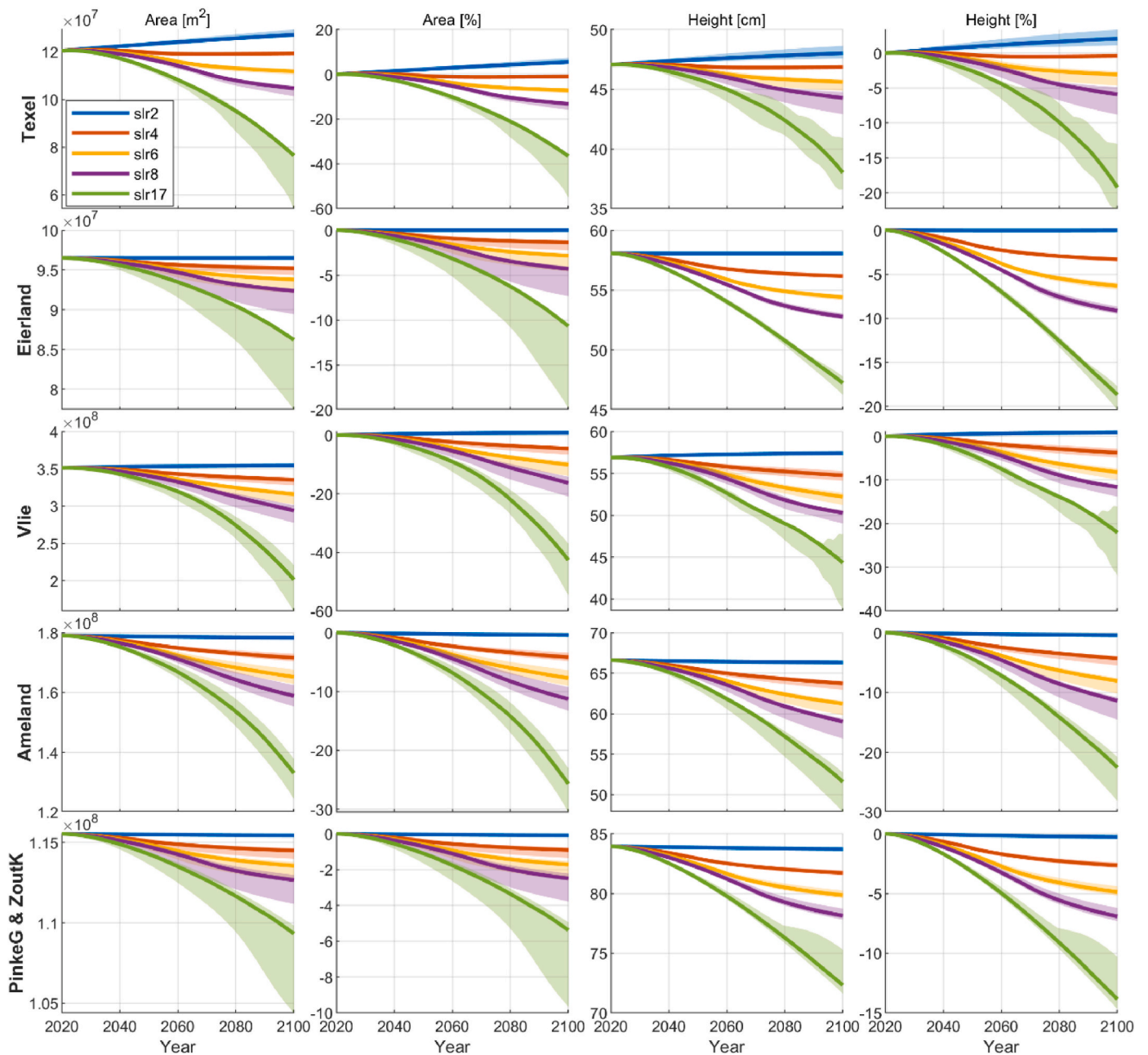
Fig. 7. Overview of the changes in intertidal area and height per basin. The y-axes are scaled differently per item and tidal inlet. Because most basins have been or are still responding to closure of Zuiderzee and Lauwerszee, the most recent curves are at one side of the bandwidth.

2100 as considered in this study and in Wang et al. (2018). Given the sensitivity of the intertidal flats to SLR, this difference in scenario likely explains a large part of the difference in loss in intertidal area. It requires further analysis to verify to which extend also differences in basin characteristics (e.g. current morphology, sediment availability and composition) and modelling approach (process based) contribute to the different estimates in area losses.

Though the estimated losses will likely have large consequences for ecology, the feared scenario of complete drowning (i.e. all intertidal flats below MLW) is not predicted by 2100 for the considered SLR rates. Given the sensitivity of the intertidal flats to the SLR-scenario and the fact that scenarios of more than 1 m SLR in 2100 are no longer inconceivable (IPCC, 2019, Table 4.6), it is important to model the full range of most recent SLR scenarios and expected land subsidence, as a follow up to this system analysis. These scenarios should preferably be combined with the probability of occurrence (Le Bars et al., 2017), as to put

the considered (extreme) scenarios in perspective. A regional update for the Netherlands of the SLR scenario's, following the recent update of global scenarios by the IPCC (2021), is expected in 2023.

4.2. Spatial differentiation among the basins

The tidal basins in the Wadden Sea will respond differently when SLR accelerates. The SLR-rate will be the same but the critical SLR-rate for drowning is very different for each basin. The critical SLR-rate reflects the ability of the basin to keep pace with SLR and depends on various basin characteristics. Firstly, the basin size determines how much sediment needs to be imported to keep pace with SLR. The larger the basin, the more sediment needs to be imported and the more difficult it will be to import enough sediment for the whole basin to keep pace with the rising sea level. Secondly, the sediment transport capacity through the inlet determines how much sediment can actually be imported. This

	SLR (mm/yr)	Volume change (m³)	Area change (m²)	height change (cm)	Volume change	Area change	Height change
Marsdiep	2	4.1E+06	6.6E+06	9.7E-01	7%	6%	2%
	4	-7.3E+05	-1.1E+06	-2.0E-01	-1%	-1%	0%
	6	-5.4E+06	-8.7E+06	-1.5E+00	-9%	-7%	-3%
	8	-9.8E+06	-1.6E+07	-2.8E+00	-17%	-13%	-6%
	17	-2.6E+07	-4.4E+07	-9.1E+00	-46%	-37%	-19%
Eierland	2	-1.2E+04	-5.3E+03	-7.9E-03	0%	0%	0%
	4	-2.8E+06	-1.3E+06	-1.9E+00	-5%	-1%	-3%
	6	-5.5E+06	-2.7E+06	-3.7E+00	-10%	-3%	-6%
	8	-8.0E+06	-4.1E+06	-5.3E+00	-14%	-4%	-9%
	17	-1.7E+07	-1.0E+07	-1.1E+01	-30%	-11%	-19%
Vlie	2	3.3E+06	3.2E+06	5.3E-01	2%	1%	1%
	4	-1.5E+07	-1.6E+07	-2.1E+00	-7%	-5%	-4%
	6	-3.1E+07	-3.5E+07	-4.7E+00	-16%	-10%	-8%
	8	-4.6E+07	-5.7E+07	-6.6E+00	-23%	-16%	-12%
	17	-9.7E+07	-1.5E+08	-1.3E+01	-49%	-43%	-22%
Ameland	2	-9.5E+05	-7.3E+05	-2.8E-01	-1%	0%	0%
	4	-9.5E+06	-7.5E+06	-2.9E+00	-8%	-4%	-4%
	6	-1.7E+07	-1.4E+07	-5.4E+00	-15%	-8%	-8%
	8	-2.4E+07	-2.0E+07	-7.6E+00	-20%	-11%	-11%
	17	-4.8E+07	-4.6E+07	-1.5E+01	-40%	-26%	-23%
Pinkegat & Zoutkamperlaag	2	-3.4E+05	-9.7E+04	-2.2E-01	0%	0%	0%
	4	-3.5E+06	-1.0E+06	-2.2E+00	-4%	-1%	-3%
	6	-6.4E+06	-2.0E+06	-4.1E+00	-7%	-2%	-5%
	8	-9.1E+06	-2.9E+06	-5.8E+00	-9%	-2%	-7%
	17	-1.8E+07	-6.2E+06	-1.2E+01	-19%	-5%	-14%

Fig. 8. Overview of changes in flat volume, area and height in 2100, for the different inlets and for the four types of sea level rise rate scenarios. The colours indicate how strong the change is, with highest losses in red and smallest losses or gains in green. (For interpretation of the references to colour in this figure legend, the reader is referred to the Web version of this article.)

Fig. 9. Graphical illustration of the results for the SLR-17 scenario, with the changes in area on the left and changes in average flat height to the right. The colours indicate how large the losses are, with the largest losses in red (>40% by 2100), the intermediate losses in orange (20%–40%) and yellow (10%–20%) and smallest losses in green (<10%). (For interpretation of the references to colour in this figure legend, the reader is referred to the Web version of this article.)

sediment transport capacity is determined by the amount of sediment that is stirred up by the waves, the tidal motion within the system and the sediment characteristics, like composition and grain size which determine how well sediment settles and erodes from the bed (represented by the vertical exchange rate in Asmita) and how well it can be transported over larger distances (represented by the horizontal exchange rate in Asmita). With finer sediments, it goes faster to transport sediment over larger distances (larger horizontal exchange rate), so it is easier for the whole basin to keep pace with the rising sea level.

Beyond the critical rate of SLR, import of sediment becomes insufficient for the tidal basin to follow the rising sea level (Stive et al., 1990; Van der Spek and Beets, 1992; Van Goor et al., 2003, Carrasco et al., 2016). As long as the SLR rate stays below the critical limit, a new dynamic equilibrium intertidal flat volume can be reached, which is smaller than its original volume. In this case, losses will occur, but complete drowning will not be the case. In Table 2, the critical SLR-rates for the six tidal basins in the Dutch Wadden Sea, as calculated by Wang et al. (2018) are presented together with the dimensionless SLR rate r

(SLR rate divided by the critical rate) for four SLR rates (2, 4, 6 and 8 mm/y). As the sediment characteristics and wave climate only vary limitedly between the basins, the critical SLR rates reflect the strong dependency on the basin size, with smaller critical rates for larger basins. For the three largest inlets, the critical rate of SLR is exceeded for the highest SLR rate considered. For this rate, these inlets are predicted to eventually drown. Timescales for complete drowning are however very large and can vary between centuries to even a millennium (Wang et al., 2018).

The calculated losses in intertidal volume (Figs. 7 and 8) are largely in line with the critical SLR rates, i.e. with smaller critical rates also more losses in volume are predicted. The Ameland inlet forms an exception. For scenarios of 4–8 mm/yr, the basin shows larger intertidal losses than the Texel inlet and comparable losses to the Vlie inlet, despite its smaller basin size and related larger critical SLR rate. Only for the highest scenario of 17 mm/yr, losses in the larger basins exceed those of the Ameland basin. This is explained by the Vlie and Texel inlet being far from their equilibrium state as a consequence of closure of the Zuiderzee (Elias et al., 2012; Wang et al., 2018). To compensate their current sediment shortage, their long-term import rates exceed the rates needed to keep pace with the current rate of SLR of 2 mm/yr. This also explains the simulated *increase* in intertidal areas for the 2 mm/yr scenario for both basins. In contrast, the Ameland basin is near equilibrium (Wang et al., 2018) and the sediment import more or less balances the amount needed to follow the current SLR rate. This means that the sediment import (and hence the sedimentation in the basin) is limited by accommodation space. Only with increasing rates in SLR, sedimentation rates will start to increase. It however takes time for the sediment import rates to increase, meaning that initially the sedimentation rates in the Ameland basin will lack behind the SLR-rate more than the sedimentation rates of the Texel and Vlie inlet. With time, the import rates to the Amelander Basin will increase. Due to its smaller basin size, less sediment is needed to grow with SLR than the Texel and Vlie inlet need. Meaning that losses in the Texel and Vlie inlet will eventually also outpace the losses in the Ameland inlet for the less extreme scenarios of 4–8 mm/yr.

As expected, the smaller basins have less difficulty keeping pace with SLR and show less volume loss (<30% for a SLR rate of 17 mm/y). These losses largely translate into loss in average height, while the volume losses in the larger basins mainly result in area changes. For the medium-sized Ameland Inlet the volume change is equally distributed over area and height. As a result, the difference in area loss is very pronounced with large losses of 26–43% for the medium and larger basins and less than 11% for the smaller basins, while the height losses stay within a range of 14–23% for all basins. The large Texel inlet even shows the smallest absolute height losses (9 cm). The relation between basin size and type of intertidal losses is determined by the shape of the hypsometric curves (Fig. 5). These reflect that the smaller basins are apparently characterized by smaller and relatively higher flats, while the larger basins are characterized by larger and relatively lower lying flats. As a result, with increasing water depth, complete areas can drown for

the larger flats, while the flats of the smaller basins more easily remain above MLW but do decrease in average height. This notion of course only applies in a general sense and cannot be used for making statement about individual intertidal flats.

By using the hypsometric curves for translating the volume changes into area and average height changes, it is assumed that the hypsometric curve does not change shape and that any sedimentation is spread evenly on the intertidal area. This does not need to be the case, as reported by Benninghoff and Winter (2019) for the German Wadden Sea. The bandwidth of the area and height changes as inferred from the historic hypsometric curves (Fig. 7) also shows that the shape of the hypsometric curve changes over time. Major causes for the historic changes are the closure of the Lauwerszee and Zuiderzee. These interventions caused abrupt and local changes to the morphology. SLR will however be a gradual and non-local change. We therefore expect that the future shape of the hypsometric curve will show less variation than observed in the past 100 years.

4.3. Spatial differentiation within the basin

To get an idea on how the loss of intertidal area is distributed within each inlet, the understanding of tidal-basin evolution under high rates of sea-level rise in the past is used. For this, analogy is made to the morphodynamic development of the transgressive Mid-Holocene Holland tidal basin in the western Netherlands under decelerating post-glacial SLR (Westerhoff and Cleveringa, 1990; Van der Spek and Beets, 1992) which exemplifies the sedimentary evolution of a tidal basin from an 'unfilled' stage to a 'filled' stage, as illustrated in Fig. 10.

The Holland tidal basin was formed in the coastal plain of the Netherlands by expansion of the North Sea and was bounded by a chain of barrier islands, separated by tidal inlets. Since the major part of the basin was not receiving sediment from debouching rivers, all the sediment had to be supplied by the North Sea coastal zone. As a result, the barrier islands were rolling over and continuously moving landwards.

In the basin, the sand imported from the North Sea was deposited near the tidal inlets as those areas were closest to the sediment source, forming partly intertidal flood-tidal deltas. Mud accumulated in the lagoon further landwards in the basin and settled in sheltered areas. With time, SLR decelerated, the basin expansion diminished, and sediment supply caught up. The flood-tidal delta's expanded, slowly filling the lagoon to intertidal level with sand.

The future of the Wadden Sea under accelerated SLR will imply the opposite situation, namely a *sediment-filled* basin under *increasing* SLR

Table 2
Critical SLR rate for drowning of the various tidal inlet systems in the Dutch Wadden Sea from (Wang et al., 2018) and the dimensionless SLR rate r for four different SLR rates (2, 4, 6 and 8 mm/yr).

Inlet	Basin Area: $A_f + A_c$ (km^2)	R_c (mm/yr)	r for SLR rate =				
			2 mm/yr	4 mm/yr	6 mm/yr	8 mm/yr	17 mm/yr
Texel	655	7.00	0.29	0.57	0.86	1.14	2.43
ELGT	158	18.0	0.11	0.22	0.33	0.44	0.94
Vlie	715	6.30	0.32	0.63	0.95	1.27	2.70
Amel	276	10.4	0.19	0.38	0.58	0.77	1.63
PinkeG	50	32.7	0.06	0.12	0.18	0.24	0.52
ZoutK	105	17.1	0.12	0.23	0.35	0.47	0.99
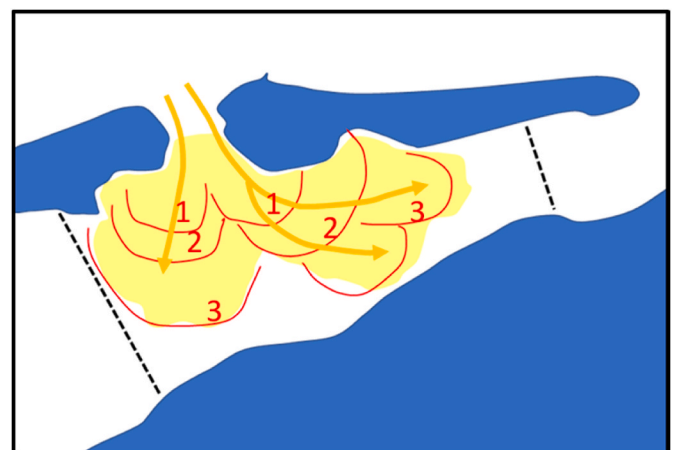
Fig. 10. Stages of development of a flood-tidal delta within a tidal basin. With infilling of the tidal basin, the delta will grow in surface area, from stage 1 to stage 2 to stage 3 (and beyond), covering an increasing part of the basin area. With a growing sand deficit, the delta will gradually become smaller in reverse order.

rates. When sediment supply to the basin falls behind on the growth in accommodation space, the basin is expected to undergo the reverse evolution. With an increasing sand deficit, the intertidal shoals in the vicinity of the inlet will remain intertidal, since all sediment is transported through the inlet, but the shoals further away will gradually receive less sand. The decline in sand supply will increase with distance from the inlet. As a result, the outer rim of the flood delta will accrete insufficiently to keep up with SLR and will gradually disappear under water. As a consequence, the flood delta starts shrinking and a subtidal lagoon develops. A basin lay-out with a flood-tidal delta near the inlet and a subtidal area surrounding it will possibly accumulate more suspended mud in its lagoon. Whether the mud will settle and accrete depends on the energy conditions in the basin. This indicates that the area just off the land reclamation works and along the western part of the tidal watershed are the most vulnerable parts for drowning of intertidal flats.

4.4. Model uncertainties

The development of intertidal flats is very sensitive to the rate of SLR. In addition, changes in mean tidal range are also expected to influence the capacity of the tidal basins to cope with SLR (Hofstede et al., 2018). The uncertainty in SLR predictions and related changes in mean tidal range forms therefore a major source of uncertainty for the estimation of future losses.

Within the ASMITA model, the uncertainty is mainly related to the model parameters for sediment transport and the equilibrium relationships. The parameters related to sediment transport, like settling rate and dispersion, have been calibrated based on their decadal response to major interventions, like the closure of the Zuiderzee and Lauwerszee (Kragtwijk et al., 2004; Van Goor et al., 2003). Because these systems have undergone a major perturbation, the sediment parameters can be well determined.

In the model, however, only one sediment fraction can be specified, representing the range of fractions that are present in reality. Especially the distinction between coarser sediments which are transported near the bed and finer sediments which are transported only in suspension is relevant. The consequence of using only one grainsize fraction, is the need for a thorough calibration, like described above. In case the two most distinct sediment classes of sand and mud are separated, the values for the sediment parameters can be derived from the sediment characteristics and length scales in these basins and need less calibration (Wang et al., 2008). It has been shown that the sand-only simulations, if properly calibrated, and the sand-mud simulations yield similar results for a rate of 6 mm/yr (Wang and Van der Spek, 2015). Therefore, the extra uncertainty introduced by working with only one fraction is regarded acceptable. However, for exploring a wider range of SLR scenarios, inclusion of mud in the model is advised.

Another uncertainty is in the equilibrium relationships. For systems that are close to equilibrium, like the Ameland inlet, these relationships can be well determined. However, for systems far out of equilibrium, like especially the case for the Texel inlet, the relationships contain great uncertainty. This results in a larger uncertainty in the absolute values for the predicted losses. It however does not affect the relative effects predicted, nor the estimated critical SLR rates, as those do not depend on the equilibrium relationships.

Differentiation within the basin cannot be made with the three-element model and is now based on system knowledge of the development of tidal basins under SLR. To improve on this, the present three-elements schematization of the ASMITA models can be extended by dividing the basins into more subparts, based on e.g. the insights from the analysis of Elias (2019). In order to do so, first the applicability of the empirical relationships for the morphological equilibrium for the subparts of the basins needs to be verified.

5. Conclusions and recommendations

Sea-level rise is expected to accelerate. This will influence the morphological development of the Wadden Sea and as a consequence its ecological functioning. In this study we explore the response of the intertidal flats to SLR, focussing on the sensitivity of the intertidal flats to the rate of SLR and on the spatial differentiation in the response. For this, simulations are carried out with the reduced-complexity model ASMITA for five SLR scenarios: one with a stable rate of 2 mm/yr (current rate), and four scenarios with accelerated SLR rates, 4, 6,8 and 17 mm/yr, for the timeframe 2020–2100.

The simulations show that the intertidal flats in the Wadden Sea are very sensitive to the SLR rate. After the SLR rate increases, it takes time for the sediment transport through the inlets to increase, which causes a sediment deficiency in the basins and a delay in deposition in the intertidal areas. As a result, the intertidal flats show an immediate response to changes in the rate of SLR. Due to the variation in the yearly averaged MSL, it may however take years to decades before these changes become noticeable. In addition, stronger rates of SLR cause larger losses. With doubling the rate of SLR the losses nearly double as well. This implies that substantially more losses may be expected for more extreme scenarios. For none of the scenarios complete drowning is predicted, though for the most extreme scenario considered (17 mm/yr), substantial relative volume losses (40%–49%) and related area losses (26–43%) are predicted for the larger basins. Area losses of 30% in the Yellow Sea coincided with observations of a strongly decreasing population of migratory birds (Studds et al., 2017).

As expected, the smaller basins have less difficulty keeping pace with SLR and show less volume losses (19–30% for a SLR rate of 17 mm/yr). Exception is the medium-sized Ameland basin, which shows comparable or even larger losses than the larger Texel and Vlie basins for scenarios of 4–8 mm/yr. Only for the highest scenario of 17 mm/yr, losses in the larger basins exceed those of the Ameland basin. The relatively large losses in the Ameland basin are explained by the basin being close to equilibrium, while the Texel and Vlie basins are still importing extra sediment in response to past engineering works. As a consequence, the sediment supply to the Ameland basin is accommodation space limited. On larger timescales, the Texel and Vlie basin are expected to also outpace the losses in the Ameland basin for the less extreme scenarios of 4–8 mm/yr. The simulated volume losses do not equally translate into losses of area and average flat height. Due to geometric differences the flats in the smaller basins mostly show a reduction in average flat height, while the flats in the larger basins mostly reduce in area. Based on the reconstruction of Holocene tidal basin evolution under high rates of SLR, it can be expected that tidal basins in the Dutch Wadden Sea will start to develop a subtidal lagoon just off the land reclamation works and along the western part of each the tidal watershed. Hence, these are the most vulnerable parts for drowning of intertidal flats.

A more quantitative estimate of the spatial differentiation within the basin can be made by dividing the basins into more elements. This however requires verifying the applicability of the empirical relationships for the morphological equilibrium for the subparts of the basins. In addition, adding a mud fraction will help to further reduce the uncertainty of the model predictions and including salt marshes will help to get a better understanding of how the vegetated intertidal areas will be able to cope with SLR.

The relevance of the evolution of the intertidal flats in response to SLR, is in its relation to ecology and safety. For this, it is valuable to carry out an integrated study, which combines the morphodynamic development with other relevant aspects, to estimate the impact on the ecology and water safety. Given the sensitivity of the intertidal flats to the rate of SLR, a broad span of possible SLR predictions should be considered, preferable combined with their likelihood of occurrence.

Declaration of competing interest

The authors declare that they have no known competing financial interests or personal relationships that could have appeared to influence the work reported in this paper.

Acknowledgements

References

Arns, A., Dangendorf, S., Jensen, J., Talke, S., Bender, J., Pattiaratchi, C., 2017. Sea-level rise induced amplification of coastal protection design heights. Scientific Reports 7 (1), 40171. https://doi.org/10.1038/srep40171.

Baart, F., Rongen, G., Hijma, M., Kooi, H., De Winter, R., Nicolai, R., 2019. Zeespiegelmonitor 2018—De stand van zaken rond de zeespiegelstijging langs de Nederlandse kust (No. 11202193-000-ZKS-0004). Deltares, Delft

Barbier, E.B., Hacker, S.D., Kennedy, C., Koch, E.W., Stier, A.C., Silliman, B.R., 2011. The value of estuarine and coastal ecosystem services. Ecological Monographs 81 (2), 169–193. https://doi.org/10.1890/10-1510.1.

Becherer, J., Hofstede, J., Gräwe, U., Purkiani, K., Schulz, E., Burchard, H., 2018. The Wadden Sea in transition—consequences of sea level rise. Ocean Dynamics 68 (1), 131–151. https://doi.org/10.1007/s10236-017-1117-5.

Beets, D.J., Van der Spek, A.J.F., 2000. The Holocene evolution of the barrier and the back-barrier basins of the Belgium and The Netherlands as a function of late Weichselian morphology, relative sea-level rise and sediment supply. Netherlands Journal of Geosciences - Geologie En Mijnbouw 79, 3–16.

Benninghoff, M., Winter, C., 2019. Recent morphologic evolution of the German Wadden Sea. Scientific Reports 9 (1), 9293. https://doi.org/10.1038/s41598-019-45683-1.

Bijsterbosch, L.W.W., 2003. Influence of Relative Sea Level Rise on Tidal Inlets (Master Thesis). Delft University of Technology, Delft, The Netherlands.

Blew, J., Südbeck, P. (Eds.), 2005. Migratory Waterbirds In the Wadden Sea 1980 – 2000. Wadden Sea Ecosystem No. 20. Wilhelmshaven, Germany: Common Wadden Sea Secretariat, Trilateral Monitoring and Assessment Group, Joint Monitoring Group of Migratory Birds in the Wadden Sea.

Buijsman, M.C., 1997. The Impact of Gas Extraction and Sea-Level Rise on the Morphology of the Wadden Sea. WL (No. Report H3099.30). Delft Hydraulics.

Carrasco, A.R., Ferreira, Ó., Roelvink, D., 2016. Coastal lagoons and rising sea level: a review. Earth-Science Reviews 154, 356–368. https://doi.org/10.1016/j.earscirev.2015.11.007.

Dam, G., van der Wegen, M., Labeur, R.J., Roelvink, D., 2016. Modeling centuries of estuarine morphodynamics in the Western Scheldt estuary. Geophysical Research Letters 43 (8), 3839–3847. https://doi.org/10.1002/2015GL066725.

Elias, E., 2019. Een actuele sedimentbalans van de Waddenzee (No. 11203683-001-ZKS-0002). Deltares, Delft.

Elias, E.P.L., 2006. Morphodynamics of Texel Inlet (PhD-Thesis). Retrieved from. http://resolver.tudelft.nl/uuid:92ad4ac0-9d54-4f5f-8536-80b7782a6aa6.

Elias, E.P.L., van der Spek, A.J.F., Wang, Z.B., de Ronde, J., 2012. Morphodynamic development and sediment budget of the Dutch Wadden Sea over the last century. Netherlands Journal of Geosciences - Geologie En Mijnbouw 91 (3), 293–310. https://doi.org/10.1017/S0016774600000457. Cambridge Core.

Eysink, W.D., 1990. Morphologic response of tidal basins to changes. In: Coastal Engineering, p. 1948. https://doi.org/10.1061/9780872627765.149, 1961.

Eysink, W.D., 1998. Effecten van bodemdaling door gaswinning in en rond de Waddenzee, Morfologie, infrastructurele en economische aspecten (No. Rapport H3099). WL | Delft Hydraulics.

Eysink, W.D., Biegel, E.J., 1992. Impact of Sea Level Rise on the Morphology of the Wadden Sea in the Scope of its Ecological Function: Investigations on Empirical Morphological Relations (No. Report H1300, Phase 3). Delft Hydraulics.

Hinkel, J., Nicholls, R.J., Tol, R.S.J., Wang, Z.B., Hamilton, J.M., Boot, G., Klein, R.J.T., 2013. A global analysis of erosion of sandy beaches and sea-level rise: an application of DIVA. Global and Planetary Change 111, 150–158. https://doi.org/10.1016/j.gloplacha.2013.09.002.

Hofstede, J.L.A., Becherer, J., Burchard, H., 2018. Are Wadden Sea tidal systems with a higher tidal range more resilient against sea level rise? Journal of Coastal Conservation 22 (1), 71–78. https://doi.org/10.1007/s11852-016-0469-1.

IPCC, 2019. In: Pörtner, H.-O., Roberts, D.C., Masson-Delmotte, V., Zhai, P., Tignor, M., Poloczanska, E., Mintenbeck, K., Alegría, A., Nicolai, M., Okem, A., Petzold, J., Rama, B., Weyer, N.M. (Eds.), IPCC Special Report on the Ocean and Cryosphere in a Changing Climate (in press).

IPCC, 2021. Climate Change 2021: the Physical Science Basis. Contribution of Working Group I to the Sixth Assessment Report of the Intergovernmental Panel on Climate Change. Cambridge University Press (in press).

Kragtwijk, N.G., 2002. Aggregated Scale Modelling of Tidal Inlets of the Wadden Sea (No. Report 22822/DC03.01.03b). WL I Delft Hydraulics/Delft Cluster, Delft, The Netherlands.

Kragtwijk, N.G., Zitman, T.J., Stive, M.J.F., Wang, Z.B., 2004. Morphological response of tidal basins to human interventions. Coastal Engineering 51 (3), 207–221. https://doi.org/10.1016/j.coastaleng.2003.12.008.

Le Bars, D., Drijfhout, S., de Vries, H., 2017. A high-end sea level rise probabilistic projection including rapid Antarctic ice sheet mass loss. Environmental Research Letters 12 (4), 044013. https://doi.org/10.1088/1748-9326/aa6512.

Lodder, Q. J., Huismans, Y., Elias, E., de Looff, H., & Wang, Z. B. (Submitted). Future Sediment Exchange between the Wadden Sea and North Sea Coast—Insights Based on ASMITA Modelling.

Lodder, Q.J., Wang, Z.B., Elias, E.P.L., van der Spek, A.J.F., de Looff, H., Townend, I.H., 2019. Future response of the Wadden Sea tidal basins to relative sea-level rise—an aggregated modelling approach. Water 11 (10). https://doi.org/10.3390/w11102198.

Nederhoff, C.M., Smits, B., Wang, Z.B., 2017. KPP Wadden, Data analyse: Getij en morfologie (No. 11200521-000-ZKS-0002). Deltares, Delft, The Netherlands.

Reed, D., van Wesenbeeck, B., Herman, P.M.J., Meselhe, E., 2018. Tidal flat-wetland systems as flood defenses: understanding biogeomorphic controls. Estuarine, Coastal and Shelf Science 213, 269–282. https://doi.org/10.1016/j.ecss.2018.08.017.

Renger, E., Partenscky, H.-W., 1974. Stability criteria for tidal basins. In: Coastal Engineering, pp. 1605–1618. https://doi.org/10.1061/9780872621138.096.

Rossington, K., Spearman, J., 2009. Past and future evolution in the thames estuary. Ocean Dynamics 59 (5), 709. https://doi.org/10.1007/s10236-009-0207-4.

Rossington, S.K., Nicholls, R.J., Stive, M.J.F., Wang, Z.B., 2011. Estuary schematisation in behaviour-oriented modelling. Marine Geology 281 (1), 27–34. https://doi.org/10.1016/j.margeo.2011.01.005.

Smaal, A.C., Nienhuis, P.H., 1992. The eastern Scheldt (The Netherlands), from an estuary to a tidal bay: a review of responses at the ecosystem level. In: Proceedings of the 26th European Marine Biology Symposium Biological Effects of Disturbances on Estuarine and Coastal Marine Environments, 30, pp. 161–173. https://doi.org/10.1016/0077-7579(92)90055-J.

Stive, M.J.F., Wang, Z.B., Ruol, P., Buijsman, M.C., 1998. Morphodynamics of a Tidal Lagoon and Adjacent Coast, vol. 397. 8th International Biennial Conference on Physics of Estuaries and Coastal Seas, The Hague, p. 407 (Conference proceedings.).

Stive, Marcel J.F., Roelvink, D.J.A., Vriend, H. J. de, 1990. Large-scale coastal evolution concept. Coastal Engineering 1990, 1962. https://doi.org/10.1061/9780872627765.150, 1974.

Stive, Marcel J.F., Wang, Z.B., 2003. Chapter 13 Morphodynamic modeling of tidal basins and coastal inlets. In: Lakhan, V.C. (Ed.), Elsevier Oceanography Series, vol. 67. Elsevier, pp. 367–392. https://doi.org/10.1016/S0422-9894(03)80130-7.

Studds, C.E., Kendall, B.E., Murray, N.J., Wilson, H.B., Rogers, D.I., Clemens, R.S., Fuller, R.A., 2017. Rapid population decline in migratory shorebirds relying on Yellow Sea tidal mudflats as stopover sites. Nature Communications 8 (1), 14895. https://doi.org/10.1038/ncomms14895.

Townend, I., Wang, Z.B., Stive, M., Zhou, Z., 2016a. Development and extension of an aggregated scale model: Part 1 – background to ASMITA. China Ocean Engineering 30 (4), 483–504. https://doi.org/10.1007/s13344-016-0030-x.

Townend, I., Wang, Z.B., Stive, M., Zhou, Z., 2016b. Development and extension of an aggregated scale model: Part 2—extensions to ASMITA. China Ocean Engineering 30 (5), 651–670. https://doi.org/10.1007/s13344-016-0042-6.

Troost, K., Ysebeart, T., 2011. ANT Oosterschelde: Long-Term Trends of Waders and Their Dependence on Intertidal Foraging Grounds (No. C063/11). Yerseke, The Netherlands: IMARES Wageningen UR. Retrieved from IMARES Wageningen UR website: https://library.wur.nl/WebQuery/wurpubs/reports/421755.

Van der Spek, A.J.F., Beets, D.J., 1992. Mid-Holocene evolution of a tidal basin in the western Netherlands: a model for future changes in the northern Netherlands under conditions of accelerated sea-level rise? Research Conference on Quaternary Coastal Evolution 80 (3), 185–197. https://doi.org/10.1016/0037-0738(92)90040-X.

Van Goor, M.A., 2001. Influence of Relative Sea Level Rise on Coastal Inlets And Tidal Basins. (No. ReportZ2822/DC03.01.03a). WL I Delft Hydraulics/Delft Cluster, Delft, The Netherlands.

Van Goor, M.A., Zitman, T.J., Wang, Z.B., Stive, M.J.F., 2003. Impact of sea-level rise on the morphological equilibrium state of tidal inlets. Marine Geology 202 (3), 211–227. https://doi.org/10.1016/S0025-3227(03)00262-7.

Van Roomen, M., Laursen, K., van Turnhout, C., van Winden, E., Blew, J., Eskildsen, K., Ens, B.J., 2012. Signals from the Wadden sea: population declines dominate among waterbirds depending on intertidal mudflats. Special Issue on the Wadden Sea Region 68, 79–88. https://doi.org/10.1016/j.ocecoaman.2012.04.004.

Vermeersen, B.L.A., Slangen, A.B.A., Gerkema, T., Baart, F., Cohen, K.M., Dangendorf, S., van der Wegen, M., 2018. sea-level change in the Dutch Wadden Sea. Netherlands Journal of Geosciences 97 (3), 79–127. https://doi.org/10.1017/njg.2018.7. Cambridge Core.

Wang, Z.B., Van der Spek, A.J.F., 2015. Importance of mud for morphological response of tidal basins to sea-level rise. In: Coastal Sediments 2015, s. vols. 1–0. WORLD SCIENTIFIC. https://doi.org/10.1142/9789814689977_0208.

Wang, Z.B., Steetzel, H., Van Koningsveld, M., 2006. Effecten Van Verschillende Scenarios Van Kustonderhoud, Resultaten Lange-termijn Simulaties Morfologische Ontwikkeling Nederlandse Noordzeekust (No. Rapport Z4051). WL | Delft Hydraulics.

Wang, Zheng, Bing, De Vriend, H.J., Stive, M.J.F., Townend, I.H., 2008. In: Dohmen-Janssen, C.M., Hulscher, S.J.M.H. (Eds.), On the Parameter Settings of Semi-empirical Long-Term Morphological Models for Estuaries and Tidal Lagoons. River, Coastal And Estuarine Morphodynamics. Taylor & Francis, pp. 103–111.

Wang, Zheng Bing, Elias, E.P.L., van der Spek, A.J.F., Lodder, Q.J., 2018. Sediment budget and morphological development of the Dutch Wadden Sea: impact of

accelerated sea-level rise and subsidence until 2100. Netherlands Journal of Geosciences 97 (3), 183–214. https://doi.org/10.1017/njg.2018.8. Cambridge Core.

Wang, Zheng, Bing, Townend, I., Stive, M., 2020. Aggregated morphodynamic modelling of tidal inlets and estuaries. Water Science and Engineering 13 (1), 1–13. https://doi.org/10.1016/j.wse.2020.03.004.

Westerhoff, W.E., Cleveringa, P., 1990. sea-level rise and coastal sedimentation in central noord-holland (The Netherlands) around 5000 BP: a case study of changes in sedimentation dynamics and sediment distribution patterns. In: Beukema, J.J., Wolff, W.J., Brouns, J.J.W.M. (Eds.), Expected Effects of Climatic Change on Marine Coastal Ecosystems. Springer Netherlands, Dordrecht, pp. 133–138. https://doi.org/10.1007/978-94-009-2003-3_17.